RSC Advances

PAPER

View Article Online
View Journal | View Issue

Cite this: *RSC Adv.*, 2019, **9**, 36144

Enhanced removal of chromium(VI) by Fe(III)-reducing bacterium coated ZVI for wastewater treatment: batch and column experiments†

Bin Zheng,[a] Yizi Ye,[b] Baowei Hu,[b] Chunhui Luo[b] and Yuling Zhu *[b]

Received 20th August 2019
Accepted 18th October 2019

DOI: 10.1039/c9ra06516d

rsc.li/rsc-advances

In order to effectively destroy the structure of the passive oxidation film that covers zero-valent iron (ZVI), an Fe(III)-reducing strain, namely *Morganella* sp., was isolated from anaerobic activated sludge and coated on ZVI, which was distributed in porous ceramsite made of iron dust, kaolin and straw, with a ratio of 7 : 3 : 1. Batch experiments showed that under the optimized conditions, the maximum removal amount of Cr(VI) by ZVI increased from 7.33 mg g^{-1} to 26.87 mg g^{-1} in the presence of the Fe(III)-reducing bacterium. The column experiment was performed with the addition of the agar globules to supply nutrients to the strain. Compared with ZVI, the column penetration time and maximum capture amount of RB-ZVI increased to 17 h and 112.5 mg g^{-1}, respectively, on the 15th day. Furthermore, the service life of RB-ZVI was prolonged in the existence of the strain. Based on X-ray diffraction, Raman spectroscopy and X-ray photoelectron spectroscopy analyses, the key mechanisms for the removal of Cr(VI) by ZVI coated with Fe(III)-reducing bacterium were determined to be adsorption, reduction, coprecipitation and biomineralization.

Introduction

Chromium (Cr) is widely applied in tanneries, printing, dyeing and galvanic industries.[1,2] Improper treatment and disposal of the industrial waste will release Cr into aquatic systems, which imposes a serious threat to all living things.[3,4] In general, two stable species of Cr, Cr(VI) and Cr(III), can be detected in the natural aquatic environment.[5] Cr(VI) is soluble, highly mobile and carcinogenic in wastewater. In contrast, Cr(III) is an essential micronutrient for human beings. It can form insoluble and less toxic precipitants, such as $Cr(OH)_3$.[6,7] Thus, the reduction of toxic Cr(VI) to the less toxic Cr(III) is a technology commonly employed in the treatment of Cr(VI)-contaminated wastewater. Many kinds of reductants have been proposed, among which zero-valent iron (ZVI) has attracted significant attention due to its low cost, high efficiency and no secondary pollutants.[8–10] ZVI-based technologies have been widely employed in the treatment of wastewater containing Cr(VI). However, some challenges still need to be addressed. During the reduction process, ZVI is gradually oxidized to iron oxides, such as Fe_2O_3, $Fe(OH)_x$ and Fe_3O_4. These form a passive film and cover the active sites on the ZVI surface, resulting in low reactivity and shortened service life.[11,12] Many efforts have been made to solve this problem, and in particular, biological methods have the advantages of high efficiency and low cost.[13,14] A type of microorganism, known as the Fe(III)-reducing bacterium, can use insoluble $Fe(OH)_x$ and Fe_2O_3 as terminal electron acceptors and yield soluble Fe(II).[15] Thus, the coating of ZVI with the Fe(III)-reducing bacterium can act as a strategy for preventing the oxidation reaction. For example, Crean *et al.* coated nanoscale palladium on the surface of biomagnetite to improve the activity of biogenic magnetite in Cr(VI) remediation.[16] Hu *et al.* immobilized *Morganella* sp. on the surface of biochar to more efficiently and conveniently remove Cr(VI) from wastewater.[17] in order to coat Fe(III)-reducing bacterium on ZVI, two factors need to be addressed. On the one hand, traditional Fe(III)-reducing bacteria are sensitive to oxygen.[18,19] Anaerobic conditions must be sustained to achieve a high biological reduction efficiency, which may inhibit the scale-up application. On the other hand, microorganisms can hardly grow on the smooth and small surface of ZVI, hence it is difficult to coat Fe(III)-reducing bacterium on ZVI.

In order to solve these two problems, a Fe(III)-reducing bacterium, *Morganella* sp., which could effectively reduce Fe(III) to Fe(II) under non-strict anaerobic conditions was selected in our laboratory. It was found that *Morganella* sp. and ZVI demonstrated synergetic effects on the removal of Cr(VI). The bacterium could hydrolyze and reduce the oxidized layer on ZVI to increase the removal efficiency of Cr(VI), but it failed to coat *Morganella* sp. on the surface of ZVI; the results were reported in

[a]*College of Economics and Management, Nanjing Forestry University, 159 Longpan Road, Nanjing, Jiangsu province, 210037, P. R. China*

[b]*School of Life Sciences, Shaoxing University, Huancheng West Road 508, Shaoxing, 312000, P. R. China. E-mail: zhuyuling@usx.edu.cn*

† Electronic supplementary information (ESI) available. See DOI: 10.1039/c9ra06516d

another paper.[20] The experiment was conducted by incubating ZVI powder and *Morganella* sp. together in a shake flask, which is not suitable for scaled-up applications.

In this study, ZVI was prepared in porous ceramsite using kaolin and straw, common agricultural waste. Following this, the bacterial strain was immobilized on ZVI with the cyclic fixing method, and the Fe(III)-reducing bacterium-coated ZVI (RB-ZVI) was obtained. Agar globules were added to the RB-ZVI to supply nutrients to the strain. Finally, batch and column experiments were carried out to evaluate the Cr(VI) removal efficiency of RB-ZVI. The mechanism was also evaluated with X-ray diffraction (XRD), Raman spectroscopy and X-ray photoelectron spectroscopy (XPS).

Experimental section

Microorganisms

Shewanella oneidensis ATCC 700550, *Shewanella decolorationis* JCM 21555, *Shewanella decolorationis* MCCC 1A11454, *Lysinibacillus* sp. VKM B-713, *Lysinibacillus* sp. JLT12, *Morganella* sp., *Bacterium* L9 and *Serratia marcescens* SW-4 were used for the selection of the Fe(III)-reducing bacterium. Detailed information on the eight strains was presented in our previous research.[17]

Screening of Fe(III)-reducing bacterium

A total of 100 mL of nutrient salt medium containing 60 mg L^{-1} $FeCl_3$ was prepared, and 2 mL of the activated strain inoculum was added under sterile conditions. The conical bottle was placed in an incubator under aerobic (shaking at 150 rpm), anoxic (static) and anaerobic (N_2) conditions, respectively. Every 24 h, the solution was withdrawn and centrifuged at 8000 rpm. The Fe(II) content in the supernatant was determined using the ferrozine method. The strain with the highest reduction efficiency for Fe(III) under anoxic condition was selected.

Preparation of RB-ZVI

Straw collected from a local farm in Lanting town, Shaoxing, Zhejiang, China was washed and dried at 60 °C. The straw was then converted into powder in order to pass through a 60-mesh screen. ZVI, kaolin and the straw powder were mixed with water in a ratio of 7 : 3 : 1 and burnt at 1000 °C for 3 h in a muffle furnace with N_2. Porous ceramsite (PC) containing ZVI was then obtained. The selected Fe(III)-reducing bacterium was activated in LB medium to prepare inoculum containing 10^7 cells mL^{-1}. A plastic column (Φ 10 cm × 20 cm) was sterilized using ultraviolet radiation for 30 min and filled with disinfected PC. The inoculum cyclically went through the PC with a speed of 10 rpm min^{-1}. The fresh inoculum was renewed every 24 h. After 15 days, the PC was withdrawn, frozen and then dried *via* a freeze dryer and RB-ZVI was thus obtained. The preparation process is demonstrated in Fig. 1. Scanning Electron Microscope (SEM) analysis was performed to observe the microscopic morphology of ZVI (PC) and RB-ZVI. The microbial community on the RB-ZVI was also evaluated to confirm the existence of the target strain.

Batch experiment

The optimal conditions for the removal of Cr(VI) in wastewater by RB-ZVI were estimated. The carbon nutrient, nitrogen nutrient and pH were optimized. For the carbon nutrient optimization, $C_6H_{12}O_6$, NaAc, sucrose and soluble starch were selected. The suitable carbon nutrient was confirmed by measuring the content of Cr(VI) in the medium every 12 h. The optimal content of the most suitable carbon nutrient was evaluated between 2 to 10 g L^{-1}. The optimal nitrogen nutrient was investigated for yeast extract powder (YE), peptone, urea and NH_4Cl. The optimum concentration of nitrogen nutrient (2, 4, 6, 8 and 10 g L^{-1}) was also determined. The pH value was optimized by controlling the pH of the solution at 4, 5, 6, 7 and 8. The effect of coexisting ions on the removal efficiency of Cr(VI) was also evaluated. Ca^{2+}, Mg^{2+}, NO_3^- and SO_4^{2-} at concentrations of 10–50 mmol L^{-1} were respectively added to the optimized medium. The residual Cr(VI) content in the solution was spectrophotometrically determined every 12 h with diphenylcarbazide.

RB-ZVI and ZVI (a total of 1 g) were added to the 200 mL optimal medium containing 200 mg L^{-1} Cr(VI). The flasks were then put in an incubator at 30 °C for 72 hours. Samples were periodically obtained and the residual concentration of Cr(VI) was measured every 12 h. The determined values were then fit to the first and second-order reaction kinetics formulas in order to compute k_1, k_2, R_1^2, R_2^2.

$$C_t/C_0 = \exp(-k_1 t), \quad (1)$$

$$C_t = C_0/(1 + k_2 C_0 t), \quad (2)$$

C_0 and C_t are the concentrations of Cr(VI) in the medium at 0 and t h, respectively.

The Cr(VI) removal amounts (q) of the RB-ZVI and ZVI were calculated and the results were matched to the pesudo-first-order (3) and pesudo-second-order kinetics (4) formulas in order to obtain the values of k_α, k_β, R_α^2, R_β^2:

$$\frac{dq}{dt} = k_\alpha(q_e - q) \quad (3)$$

$$\frac{dq}{dt} = k_\beta(q_e - q)^2 \quad (4)$$

where q_e was the maximum removal quantity.

Column experiment

The agar globules were prepared based on the optimal carbon and nitrogen nutrient concentrations achieved from the batch experiment. Carbon and nitrogen sources (10× optimized concentration) were fixed in 20% agar *via* a small ball model (Φ = 1 cm). Subsequently, 200 g of RB-ZVI and 40 g agar globules were mixed and loaded into an adsorption column (40 cm × 5 cm). The solution containing 70 mg L^{-1} Cr(VI) was passed through the filler with a speed of 20 rpm. The residual content of Cr(VI) in the effluent was detected every 30 min and the penetration curve was determined. The solution was replaced by a solution containing 35 mg L^{-1} Cr(VI) after the adsorption

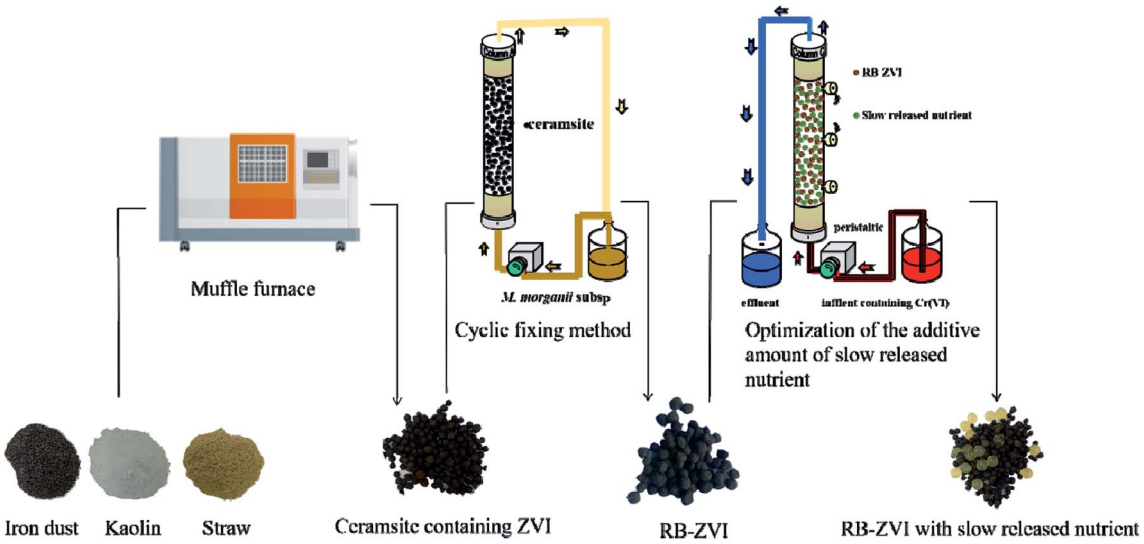

Fig. 1 The preparation process for RB-ZVI.

column was penetrated, and was changed every 24 h. The penetration curves were determined on the 5th, 10th and 15th days. The obtained values were matched to the logistic model (5) to calculate the penetration time,[21] and to the Thomas formula to calculate the maximum adsorption amount (6).[22] ZVI was used as a control. The DNA of the samples from the RB-ZVI column was extracted *via* an OMEGA kit, and the V3–V4 region was amplified by primers 341F and 805R. High throughput sequencing analysis was then carried out at Shanghai Biotech Co. (Shanghai, China).

$$\frac{C}{C_0} = 1 - \frac{1}{1 + \left(\frac{t}{t_0}\right)^p} \quad (5)$$

p is the slope of the penetration curve, and t_0 is the penetration time (h).

$$\frac{C}{C_0} = \frac{1}{1 + \exp\left(\frac{k_{Th}}{Q} q_{Th} m - k_{Th} C_0 t\right)} \quad (6)$$

k_{Th} is the rate coefficient (mL min^{-1} mg^{-1}), q_{Th} is the maximum removal capacity (mg g^{-1}), m is the weight of RB-ZVI or PC in the column (g), t is the efflux time (min), and Q is the flow rate (mL min^{-1}).

Characterization

XRD, Raman spectroscopy and XPS analyses were applied to characterize the change in ZVI in the presence and absence of the Fe(III)-reducing bacterium. After reaction with Cr(VI), ZVI was filtered, washed three times, then vacuum dried and preserved before analysis.

Results and discussion

Screening of Fe(III)-reducing bacterium

The reduction efficiency of Fe(III), *via* eight strains under anoxic and anaerobic conditions, is displayed in Fig. 2. Notably, under anoxic conditions, the Fe(III) reduction efficiency of *Morganella* sp. was higher than that of the other 7 strains, reaching 64.3 ± 3.2% in 24 h and 100% in 48 h. In accordance with the previously reported results, bacteria belonging to the *Shewanella* genus (strain 1–strain 3) demonstrate a more positive reduction effect under anaerobic conditions than those in an anoxic environment.[23,24] *Morganella* sp. also exhibited a high reduction efficiency under the anoxic conditions. A possible explanation is that the Fe(III) reduction efficiency of *Morganella* sp. was not sensitive to oxygen. It could transform Fe(III) into Fe(II) under both anaerobic and anoxic conditions, which is more suitable for scale-up applications. Previously, Hu *et al.* found that Cr(VI) was efficiently reduced to Cr(III) by *Morganella* sp. The data presented here show that it could transform Fe(III) into Fe(II), which demonstrates that the strain possesses metal reduction ability.[17] It was also reported that *Morganella* sp. could efficiently decolorize and degrade azo dyes and has great potential in pollution control.[25,26] Thus, *Morganella* sp. was selected as the Fe(III)-reducing bacterium for further study.

Preparation of RB-ZVI

ZVI, kaolin and straw, in the ratio of 7 : 3 : 1 (g : g : g), were used to prepare porous ceramsite; kaolin was the support and straw powder was burned to ash to form pores. The ratio of ZVI to kaolin to straw powder was optimized by investigating five ratios, *i.e.*, 9 : 1 : 1; 8 : 2 : 1; 7 : 3 : 1; 6 : 4 : 1; 5 : 5 : 1. With the ratios of 9 : 1 : 1 and 8 : 2 : 1, the circular bobble was not obtained because of the low concentration of kaolin. With the ratios of 6 : 4 : 1 and 5 : 5 : 1, the Cr(VI) removal efficiency of the obtained ceramsite was lower than that of 7 : 3 : 1 due to the lower porosity and lower ZVI content. After cyclic fixing, *Morganella* sp. was immobilized on ZVI in pore ceramsite and RB-ZVI was obtained. The surface morphology and the structure of ZVI and RB-ZVI were characterized *via* SEM, with the results presented in Fig. 3. Well developed pores were observed on the ceramsite, which supplied growth space for *Morganella* sp. ZVI

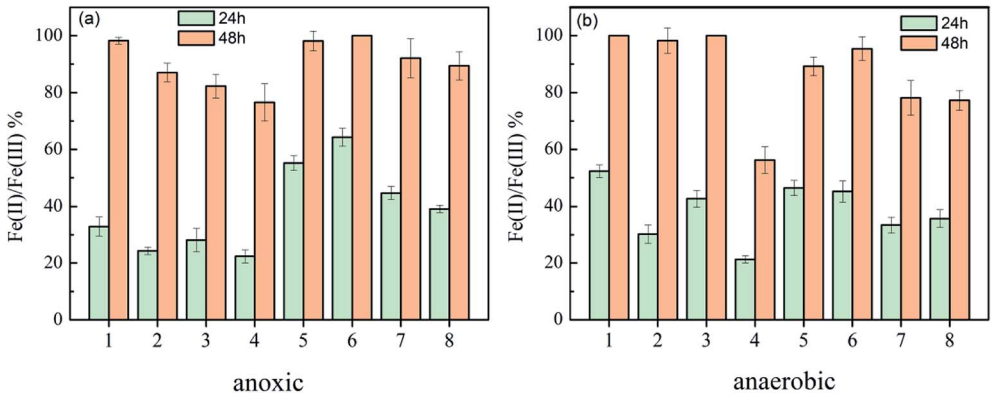

Fig. 2 The Fe(III) reduction efficiency of the eight strains under anoxic (a) and anaerobic (b) conditions. 1–8: *S. oneidensis* ATCC 700550, *S. decolorationis* JCM 21555, *S. decolorationis* MCCC 1A11454, *Lysinibacillus* sp. VKM B-713, *Lysinibacillus* sp. JLT12, *Morganella* sp., *Bacterium* L9 and *S. marcescens*.

was distributed in ceramsite with a rough surface, providing an immobilization area for the strain. In RB-ZVI, *Morganella* sp. grew on the pores, demonstrating that microorganisms were successfully fixed on the ZVI.

To further confirm whether *Morganella* sp. was immobilized on ZVI, high throughput sequencing was conducted to evaluate the cultures grown on RB-ZVI. As exhibited in Fig. 4, the dominant phylum was *Proteobacteria* and the main class was *Gammaproteobacteria*. In addition, the predominant order was determined to be *Enterobacteriales*, with *Enterobacteriaceae* as the main family. However, the dominant main genus was unclassified, which meant that it was a new genus in the database. The classifier from the phylum to the family of the predominant strain was in accordance with *Morganella* sp. The results confirmed that *Morganella* sp. was involved in RB-ZVI. In addition to *Morganella* sp., strains belonging to other genera were also detected as the microorganisms in the air and may have been involved in the fixing process. However, they were not dominant species in ZVI. It must also be mentioned that the relative abundance of the dominant genus in RB-ZVI increased after the treatment of wastewater containing Cr(VI). This indicates that *Morganella* sp. could become the predominant strain in the process of Cr(VI) removal.

Batch experiment

The nutrient for the removal of Cr(VI) with RB-ZVI was optimized and the results are shown in Fig. 5. In the first 24 h, the microorganism concentration was low and ZVI played the major role in the removal of Cr(VI). The carbon nutrient significantly affected the removal efficiency of Cr(VI) in the next 24 h. When $C_6H_{12}O_6$ was employed as the carbon nutrient, 92.0% of Cr(VI) was removed in 48 h. The removal efficiency was observed as 51.0%, 28.0%, 34.6% and 54.3%, respectively, in the presence of LB, sodium acetate, starch and sucrose. For RB-ZVI, 4 g L^{-1} of $C_6H_{12}O_6$ was optimal. Likewise, the nitrogen nutrient displayed a significant impact on the Cr(VI) removal efficiency. Among the 5 types of nitrogen nutrients, YE was optimal for RB-ZVI. A removal efficiency of 100% was achieved when YE was used as the nitrogen nutrient. The concentration of YE was also optimized and a content of 6 g L^{-1} was most suitable for RB-ZVI. Furthermore, pH was also a crucial factor for the performance of RB-ZVI. In the acidic solution, the Cr(VI) removal rate was reduced. A removal efficiency of 100% was achieved at the pH of 7.

The effect of coexisting ions on the removal efficiency of Cr(VI) is shown in Fig. S1.† It can be seen that SO_4^{2-} and NO_3^- in the concentration range of 10–50 mmol L^{-1} did not demonstrate

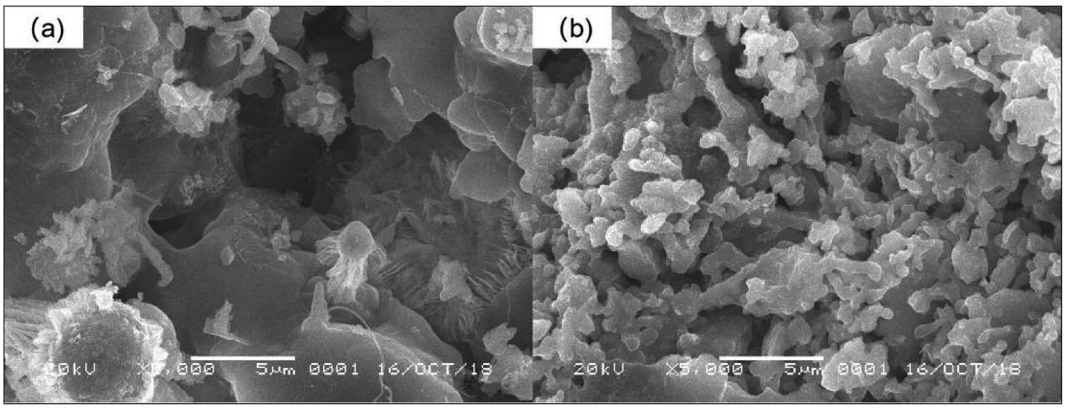

Fig. 3 SEM analysis of ZVI (a) and RB-ZVI (b).

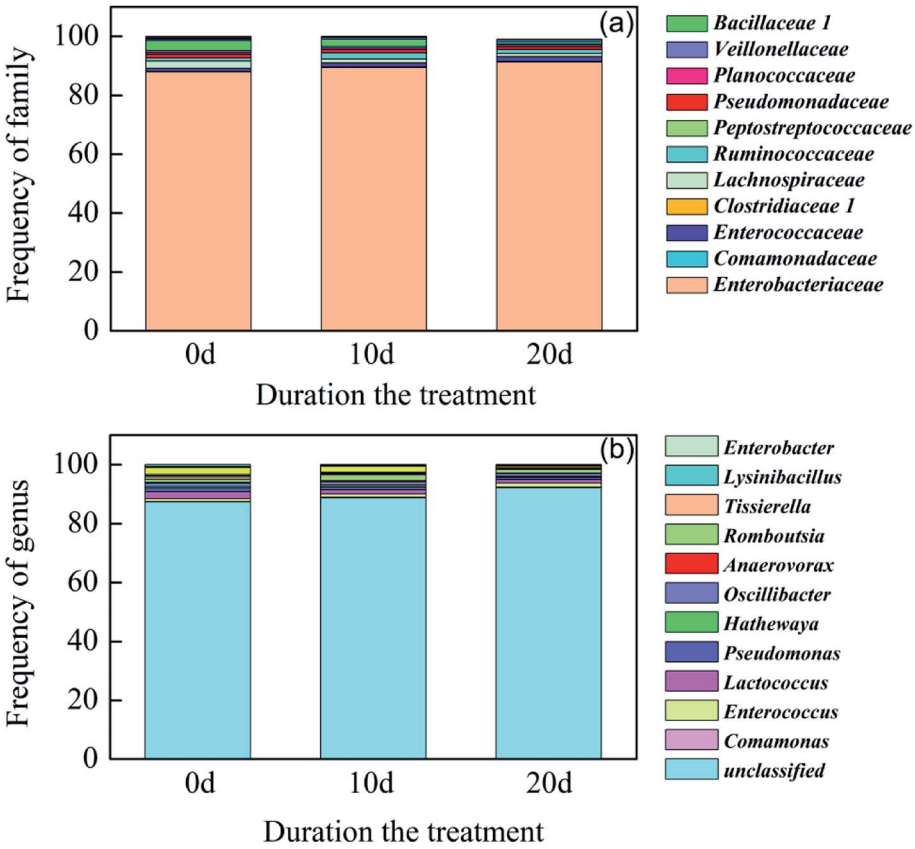

Fig. 4 Microorganisms involved in the RB-ZVI column before and after running with a solution containing Cr(VI). (a) At the family level and (b) at the genus level.

significant effects on removing Cr(VI) from wastewater; however, Ca^{2+} and Mg^{2+} increased the removal efficiency. Without Ca^{2+} or Mg^{2+}, about 67.3% of Cr(VI) was removed in 36 h. In the presence of 30 mmol L^{-1} Ca^{2+} or Mg^{2+}, about 84.2% or 82.1% of Cr(VI) was captured in 36 h, respectively. It was reported that Ca^{2+} and Mg^{2+} in the solution could increase the activity of metal reductase, and thus raise the removal efficiency of Cr(VI).[27]

Kinetics analysis was conducted to compare the removal efficiencies of ZVI and RB-ZVI. As illustrated in Fig. 6, the concentration of Cr(VI) decreased dramatically in the first 12 h. Adsorption and chemical reduction played important roles in this period.[28] The residual concentration was maintained relatively steady for the following 60 h. This may be attributed to the low level of active sites on ZVI after 12 h, leading to the minimal removal of Cr(VI). When RB-ZVI was used to capture Cr(VI) from wastewater, a significant decline of the Cr(VI) content appeared in the first 12 h, followed by a decrease in the Cr(VI) content at a higher rate. The reason may be that adsorption and chemical reduction were the initial reactions, followed by the growth of the Fe(III)-reducing bacterium. The hydrolysis enzyme was then yielded to remove the passive film covering ZVI, thereby leading to the release of active sites.[29] Thus, compared with ZVI, RB-ZVI removed more Cr(VI) from the wastewater.

The first and second-order kinetics equations were employed to compute the Cr(VI) removal rates of ZVI and RB-ZVI, respectively. The calculated results are reported in Table S1.† Poor fits were observed between the kinetic formulas and the ZVI system, with R^2 values of 0.726 and 0.749. This may be due to the long reaction time. However, the first-order kinetics formula presented an improved fit with the RB-ZVI removal system, with an R^2 value of 0.968. This implies that the mechanisms involved in RB-ZVI are distinct from those in ZVI, with the Fe(III)-reducing bacterium demonstrating a positive impact on the improvement of ZVI activity.[27]

To further evaluate the synergistic effect in the RB-ZVI system, the removal mass of Cr(VI) *via* ZVI in the presence and absence of Fe(III)-reducing bacterium was calculated and fit to the pseudo-first and second-order kinetics formulas, (3) and (4), respectively. As demonstrated in Table S2,† the process of Cr(VI) removal by ZVI can be well described *via* the pseudo-second-order kinetics formula, with an R^2 value of 0.986. However, the pseudo-first-order kinetics was more suitable for the PRB-ZVI process. In the presence of Fe(III)-reducing bacterium, the maximum removal ability of ZVI increased from 7.33 mg g^{-1} to 26.87 mg g^{-1}, indicating that the strain can promote the removal of Cr(VI) and that RB-ZVI has tremendous potential for such applications.

Column experiment

Based on the batch experiment, a column test was performed to evaluate the potential application of RB-ZVI. Agar globules

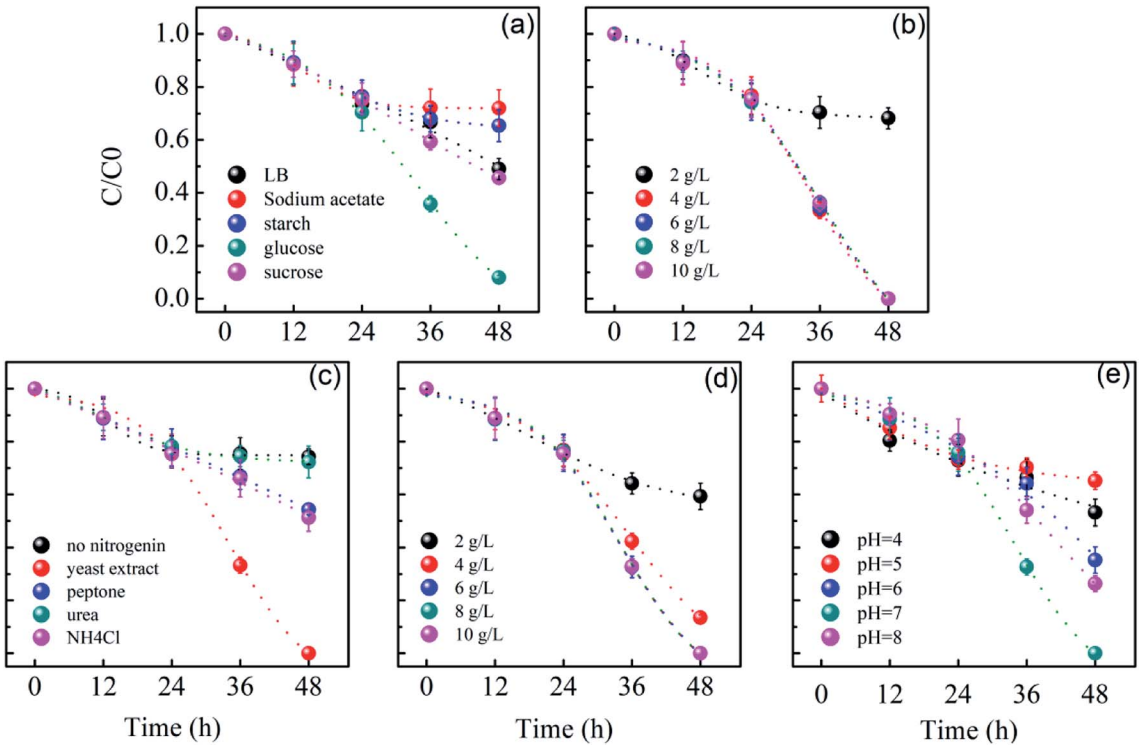

Fig. 5 Effects of carbon nutrient (a), carbon nutrient content (b), nitrogen nutrient (c), nitrogen nutrient content (d) and pH (e) on the removal of Cr(VI) *via* RB-ZVI.

containing $C_6H_{12}O_6$ of 40 g L^{-1} and YE of 60 g L^{-1} were immobilized in a 20% agar ball, which supplied carbon and nitrogen sources for Fe(III)-reducing bacterium. The amount added was also optimized and the results demonstrated that the highest Cr(VI) removal efficiency was achieved with 200 g RB-ZVI and 40 g agar globules. Moreover, an excess of nutrients resulted in the release of carbon and nitrogen nutrients into the wastewater. The COD content, total nitrogen (TN) and total phosphorus (TP) in the effluent were also detected (data not shown). The results showed that approximately 186.2 mg L^{-1} COD, 0.78 mg L^{-1} TN and 0.08 mg L^{-1} TP were released, respectively, after running for 30 days, meeting the sewage discharge level 2 standard in China.

A column experiment was conducted in plexiglass columns (40 cm × 5 cm) filled with RB-ZVI (or ZVI) and agar globules at a ratio of 50 : 1. The penetration curves were determined on days 1, 5, 10 and 15. Data on the content of Cr(VI) was collected at an interval of 0.5 h and fitted to the logistic eqn (5) to determine the penetration time (Fig. 7). In addition, the Thomas eqn (6) was used to calculate the adsorption amounts

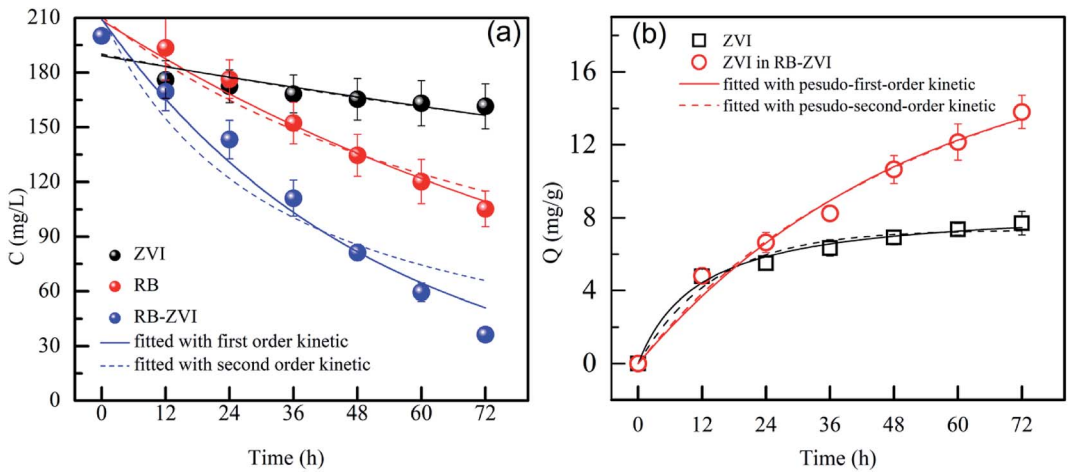

Fig. 6 Kinetics analysis of the removal process: (a) fitted with first and second-order dynamics formulas; (b) fitted with pseudo-first and second-order dynamics formulas.

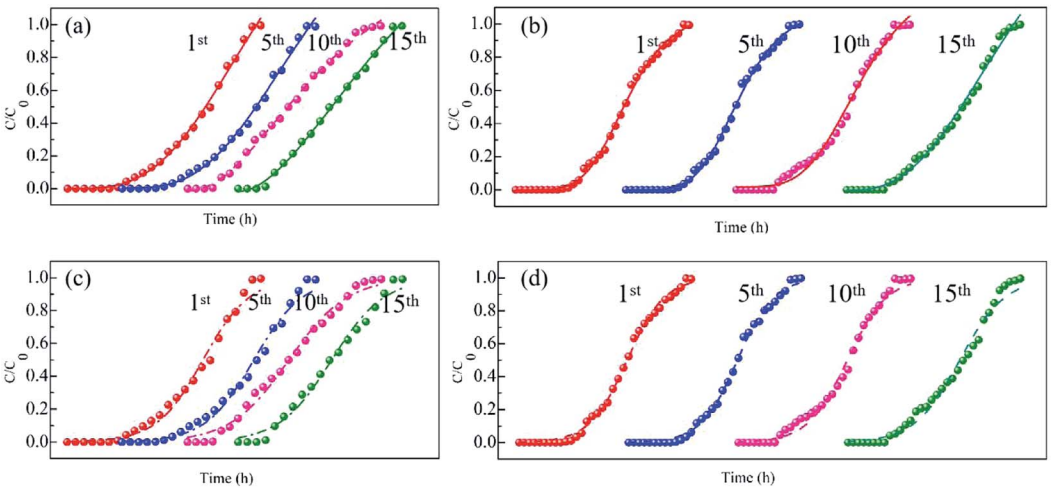

Fig. 7 The penetration curves of ZVI (a and b) and RB-ZVI (c and d) running on days 1, 5, 10 and 15. (a and c) Fitted with the logistic model; (b and d) fitted with the Thomas model.

of RB-ZVI and ZVI (Table S3†). ZVI was saturated faster, with the penetration time and adsorption capacity of 11.8 h and 85.5 mg g^{-1}, respectively, on the first day and the corresponding values of 8.6 h and 53.7 mg g^{-1} on the 15th day. The penetration time and adsorption amount of ZVI both declined with the increased reaction time. This can be attributed to the passive film formed by substances such as Fe_2O_3 and $Fe(OH)_x$ covering the surface of ZVI, leading to a lower removal efficiency.[12,30]

Compared with ZVI, the adsorption capacity of RB-ZVI drastically increased, with the maximum removal amount of 108.9 mg g^{-1} on day 1 and 112.5 mg g^{-1} on day 15. In addition, the penetration time increased from 10.7 h to 17 h after 15 days of operation. To explain this observed phenomenon, it was assumed that extracellular polymer secreted by Fe(III)-reducing bacterium could adsorb Cr(VI) on day 1. The microorganisms in RB-ZVI then grew and yielded the hydrolysis enzyme, which could hydrolyze the passive film by reducing Fe(III) to Fe(II). On the other hand, as the reaction proceeded, *Morganella* sp. acclimated to the environment containing Cr(VI) and grew rapidly, which resulted in the enhanced removal ability of RB-ZVI.[31,32] Our findings also suggest that agar globules could supply sufficient carbon and nitrogen nutrients to the Fe(III)-reducing bacterium and prolong the usage life of RB-ZVI.

Mechanism

XRD analysis. XRD measurements of the samples in the absence and presence of *Morganella* sp. were carried out to determine the crystal structure change of ZVI (Fig. 8). In the absence of *Morganella* sp., no obvious differences in peaks were observed between the ZVI samples on treating Cr(VI) for 24 h and 48 h. Three peaks at approximately 45.6°, 65.1° and 82.4° represent the cubic phases of Fe(0).[33] The results imply that the removal of Cr(VI) occurred in the first 24 h, and no significant difference appeared in the following 24 h. Moreover, in the presence of *Morganella* sp., the XRD patterns of ZVI collected at 24 h were similar to those of the single ZVI system. However, a secondary mineral phase, corresponding to the peak at 32.2°, was present in the ZVI products obtained at 48 h. According to previous reports, the secondary mineral may have been produced from FeOOH and Fe(II), which could incorporate Cr(VI) into the iron ore.[34,35]

Raman analysis. In order to confirm the presence of the new mineral, the non-crystal structural change in ZVI was further studied with Raman spectroscopic. In the absence of the Fe(III)-reducing bacterium, no significant changes in the new iron phase were observed following 24 h and 48 h of Cr(VI) treatment for ZVI. Fig. 9a and b show peaks at 380 cm^{-1} and 1304 cm^{-1}, which can be attributed to lepidocrocite. In addition, a peak assigned to magnetite at 668 cm^{-1} was also observed. This implies that FeOOH and Fe_3O_4 appeared in the removal process and covered the surface of ZVI. This result is in agreement with Montesinos *et al.*[36] and Liang *et al.*,[37] both of whom demonstrated that lepidocrocite and magnetite appeared on the surface of ZVI in the aging process and formed a passive outer

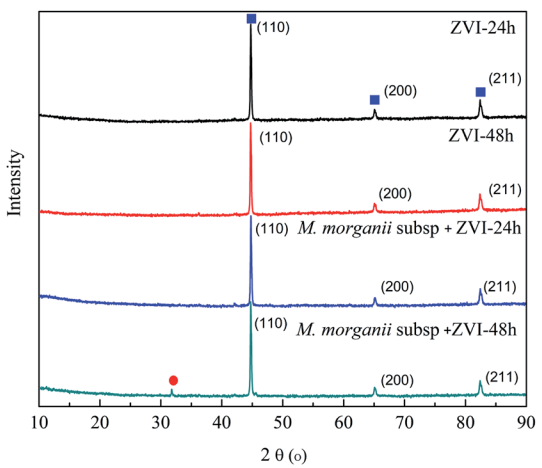

Fig. 8 XRD patterns of Cr(VI)-treated ZVI and RB-ZVI samples collected at 24 h and 48 h.

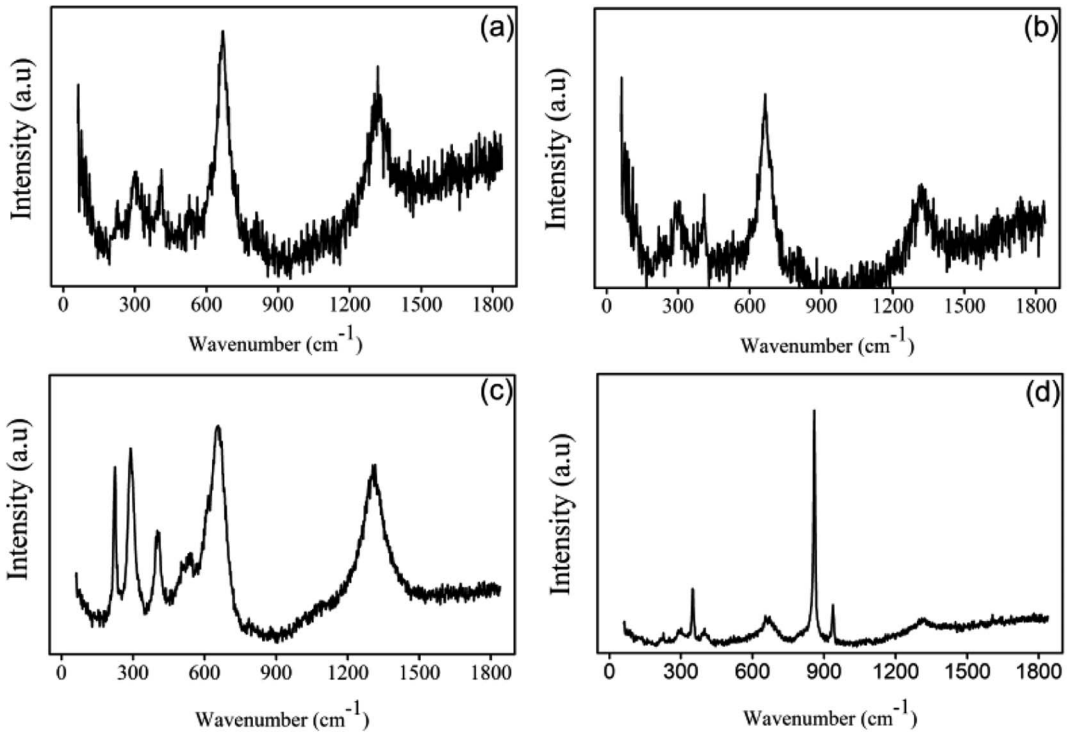

Fig. 9 Raman spectra of Cr(VI)-treated ZVI and RB-ZVI samples collected at 24 h and 48 h. (a) Cr(VI)-treated ZVI-24 h, (b) Cr(VI)-treated ZVI-48 h, (c) Cr(VI)-treated RB-ZVI-24 h and (d) Cr(VI)-treated RB-ZVI-48 h.

layer. With the Fe(III)-reducing strain, lepidocrocite and magnetite were detected at 24 h and decreased significantly at 48 h. Four new sharp peaks at 930 cm^{-1}, 843 cm^{-1}, 688 cm^{-1} and 363 cm^{-1} appeared. The peak at 688 cm^{-1} was attributed to $FeCr_2O_4$, which implies that coprecipitation occurred in the removal process.[38] The peaks at 843 cm^{-1} and 930 cm^{-1} can be assigned to the ν Fe=O bond and Cr–O bond, respectively, possibly in the structure of the newly formed mineral.[39,40] The new mineral did not appear in the Raman spectra of ZVI in the absence of the Fe(III)-reducing bacterium, confirming that *Morganella* sp. could biomineralize Cr and Fe to yield the Cr–Fe mineral.

XPS analysis. XPS was applied to characterize the state of Cr and Fe on the surface of ZVI and RB-ZVI after the treatment of Cr(VI)-containing wastewater (Fig. 10). The binding energy shifts were detected and the deconvolution of Fe 2p and Cr 2p peaks were analyzed using the XPSPEAK 41 software. In the spectra of ZVI, the observed peaks at 710.1 eV and 717.7 eV are attributed

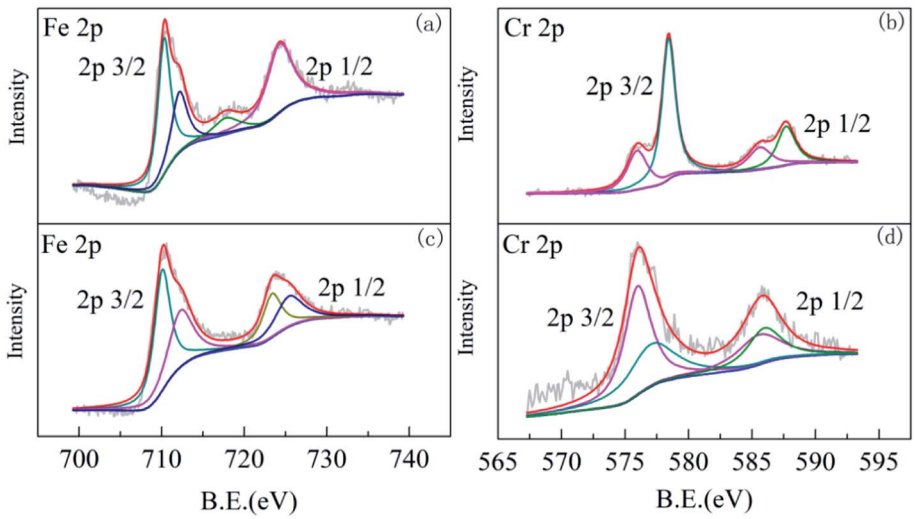

Fig. 10 Cr 2p (a) and Fe 2p (b) XPS spectra of Cr(VI)-treated ZVI. Cr 2p (c) and Fe 2p (d) XPS spectra of Cr(VI)-treated RB-ZVI.

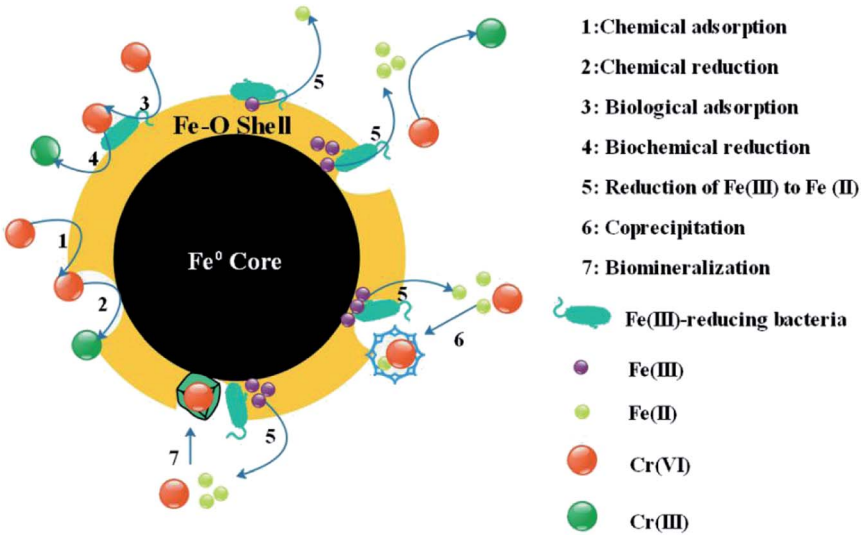

Fig. 11 The proposed Cr(VI) removal mechanism of RB-ZVI.

to Fe(0),[41] and the peaks present at 712.3 eV and 724.4 eV are characteristic of Fe(II) and FeOOH.[42,43] This implies that the passive film covered the Fe(0) surface. Moreover, two predominant peaks at 578.45 eV and 587.74 eV assigned to Cr(VI) were observed. Two additional peaks (575.97 eV and 585.69 eV) with lower intensities, in accordance with Cr(III), were also present.[44,45] Clearly, Cr(VI) is the major chemical present in ZVI. For RB-ZVI, it is worth mentioning that besides Fe(0), Fe(II) peaks at 712.2 eV and 725.3 eV were also determined.[46] In addition, the content of Cr(III) was higher than that of Cr(VI). Due to the effect of the Fe(III)-reducing strain, FeOOH was hydrolyzed to Fe(II), releasing the active site of Fe(0) and reducing Cr(VI) to Cr(III).

Possible removal mechanism of Cr(VI) with RB-ZVI. According to the above analysis and our previous research,[20] the Cr(VI) removal mechanism with RB-ZVI was proposed and demonstrated in Fig. 11. In the initial period, Cr(VI) was removed with ZVI through adsorption and reduction. The active sites were covered with a passive film formed by Fe_3O_4 and FeOOH, resulting in decreased removal efficiency. *Morganella* sp. could also adsorb Cr(VI) *via* extracellular polymers. The strain then grew, utilized the carbon and nitrogen sources released from the nutrient, and reduced Fe(III) in Fe_3O_4 and FeOOH to Fe(II). This caused the removal of the passive film covering ZVI. The produced Fe(II) further reduced Cr(VI) to Cr(III), leading to the high removal efficiency of Cr(VI). Cr(III) was present in RB-ZVI in the form of Cr_2O_3 and a new mineral. This implies that besides adsorption and reduction, co-precipitation and biomineralization, which were caused by the second mineralization of FeOOH and Fe(II), were also involved in the removal process.[47–49]

Conclusion

In this work, a new Fe(III)-reducing bacterium, *Morganella* sp., which could transform Fe(III) to Fe(II) with higher efficiency than *Shewanella* under anoxic condition, was selected. The Fe(III)-reducing bacterium was then coated on porous ceramsite made of ZVI, kaolin and straw with a ratio of 7 : 3 : 1 in order to prepare RB-ZVI. Batch experiments demonstrated that the maximum removal amount of Cr(VI) *via* RB-ZVI increased from 7.33 mg g^{-1} to 26.86 mg g^{-1} under the optimal conditions of 4 g L^{-1} $C_6H_{12}O_6$, 6 g L^{-1} YE and a pH of 7. Column testing showed that the penetration time and maximum adsorption amount increased to 17 h and 112.5 mg g^{-1}, which were significantly enhanced with *Morganella* sp. The mechanism of the removal of Cr(VI) *via* RB-ZVI was then investigated with XRD, Raman and XPS. The results showed that four main mechanisms, adsorption, reduction, coprecipitation and biomineralization, were involved in the removal process. This evidence confirmed that the Fe(III) reducing bacterium can increase the removal efficiency of ZVI under experimental conditions. The prepared RB-ZVI can be potentially employed in the treatment of Cr(VI) contaminated wastewater.

Conflicts of interest

There are no conflicts to declare.

Acknowledgements

Project Supported by the National Natural Science Foundation of China (Grant No. 71603118).

References

1 J. X. Shi, B. G. Zhang, R. Qiu, C. Y. Lai, Y. F. Jiang, C. He and J. H. Guo, *Environ. Sci. Technol.*, 2019, **53**, 3198–3207.
2 N. Zhao, Z. Ying, F. Liu, M. Zhang, Y. Lv, Z. Hao, G. Pan and J. Pan, *Bioresour. Technol.*, 2018, **260**, 294–301.
3 H. He, Z. Xiang, H. Chen, X. Chen, H. Huang, M. Wen and C. Yang, *Int. J. Environ. Sci. Technol.*, 2018, **15**(7), 1491–1500.

4 S. Dey and A. K. Paul, *Int. Biodeterior. Biodegrad.*, 2018, **132**, 122–131.
5 S. Norouzi, M. Heidari, V. Alipour, O. Rahmanian, M. Fazlzadeh, F. Mohammadi-moghadam, H. Nourmoradi, B. Goudarzi and K. Dindarloo, *Bioresour. Technol.*, 2018, **258**, 48–56.
6 P. Miretzky and A. F. Cirelli, *J. Hazard. Mater.*, 2010, **180**(1–3), 1–19.
7 T. Shi, D. Yang, H. Yang, J. Ye and Q. Cheng, *Appl. Clay Sci.*, 2017, **142**, 100–108.
8 P. Feng, X. Guan and Y. Sun, *J. Environ. Sci.*, 2015, **31**(5), 175–183.
9 C. J. Lin and S. L. Lo, *Water Res.*, 2005, **39**(6), 1037–1046.
10 M. Gheju, *Water, Air, Soil Pollut.*, 2011, **222**(1–4), 103–148.
11 A. M. Moore, C. H. Leon and T. M. Young, *Environ. Sci. Technol.*, 2003, **37**(4), 3189–3198.
12 X. H. Guan, Y. Sun, H. Qin, J. Li, I. M. Lo, D. He and H. R. Dong, *Water Res.*, 2015, **75**, 224–248.
13 B. G. Zhang, S. Wang, M. H. Diao, J. Fu, M. M. Xi, J. X. Shi, Z. Q. Liu, Y. F. Jiang, X. L. Cao and A. G. L. Borthwick, *J. Geophys. Res.: Biogeosci.*, 2019, **124**, 601–615.
14 B. G. Zhang, Y. T. Cheng, J. X. Shi, X. Xing, Y. L. Zhu, N. Xu, J. X. Xia and A. G. L. Borthwick, *Chem. Eng. J.*, 2019, **375**, 121965.
15 M. Gan, P. He, C. Y. Gu, Z. H. Zheng, J. Y. Zhu, S. Zhou, X. X. Liu and G. Z. Qiu, *Int. Biodeterior. Biodegrad.*, 2019, **137**, 78–87.
16 D. E. Crean, V. S. Coker, G. Laan and J. R. Lloyd, *Environ. Sci. Technol.*, 2012, **46**, 3352–3359.
17 B. W. Hu, Y. Z. Song, S. Y. Wu, Y. L. Zhu and G. D. Sheng, *J. Mol. Liq.*, 2019, **286**, 110876.
18 S. E. Childers, S. Ciufo and D. R. Lovley, *Nature*, 2002, **416**(6882), 767–769.
19 N. T. Van, F. Lieben and J. Dries, *Environ. Sci. Technol.*, 2007, **41**, 5724–5730.
20 J. M. Huang, Y. Z. Ye, Z. Fu, W. J. Dun, Y. Y. Wang, L. S. Fang, S. H. Ye, X. Y. Ye, J. J. Jin, Q. Y. Hu and Y. L. Zhu, *Nat., Environ. Pollut. Technol.*, 2019, **18**(3), 871–877.
21 G. Yan, T. Viraraghavan and M. Chen, *Adsorpt. Sci. Technol.*, 2001, **19**, 25–43.
22 P. Rout, P. Bhunia and R. Rajesh, *J. Water Process Eng.*, 2017, **17**, 168–180.
23 X. Xiao, C. C. Xu, Y. M. Wu, P. J. Cai and H. Q. Yu, *Bioresour. Technol.*, 2012, **110**, 86–90.
24 G. Y. Wang, B. G. Zhang, S. Li, M. Yang and C. C. Yin, *Bioresour. Technol.*, 2017, **227**, 353–358.
25 H. Pathak, D. Soni and K. Chauhan, *Chemosphere*, 2014, **105**, 126–132.
26 Z. Ergul-Ulger and A. D. Ozkan, *Sep. Sci. Technol.*, 2014, **49**(6), 907–914.
27 D. J. Opperman, L. A. Piater and E. v. Heerden, *J. Bacteriol.*, 2008, **190**(8), 3076–3082.
28 L. Sun, Z. Yuan, W. Gong, L. Zhang, Z. Xu, G. Su and D. Han, *Appl. Surf. Sci.*, 2015, **328**, 606–613.
29 Z. H. Ai, Y. Cheng, L. Z. Zhang and J. R. Qiu, *Environ. Sci. Technol.*, 2008, **42**, 6955–6960.
30 L. Chen, S. Jin and P. H. Fallgren, *J. Hazard. Mater.*, 2012, **239–240**(5), 265–269.
31 S. Ozturk, T. Kaya, B. Aslim and S. Tan, *J. Hazard. Mater.*, 2012, **15**, 64–69.
32 T. Joutey, W. Bahafid, H. Sayel, S. Anaou and E. Ghachtouli, *Environ. Sci. Pollut. Res. Int.*, 2014, **4**, 3060–3072.
33 Y. K. Sun, Y. D. Song, J. L. Qiao, B. C. Pan, W. M. Zhang and X. H. Guan, *Chem. Eng. J.*, 2018, **354**, 445–453.
34 D. E. Latta, C. A. Gorski and M. M. Scherer, *Biochem. Soc. Trans.*, 2012, **40**, 1191–1197.
35 N. F. Papassiopi, M. Pinakidou, G. S. Katsikini, C. Antipas, A. Christou and E. C. Paloura, *Chemosphere*, 2014, **111**, 169–176.
36 V. N. Montesinos, Q. Natalia, E. B. Halac, G. L. Ana, C. Graciela, B. Silvina, Z. Guillermo and I. L. Marta, *Chem. Eng. J.*, 2014, **244**, 569–575.
37 L. Liang, X. Guan, Z. Shi, J. Li, Y. Wu and P. G. Tratnyek, *Environ. Sci. Technol.*, 2014, **48**, 6326–6334.
38 M. Chen, J. F. Shu, X. D. Xie and H. K. Mao, *Geochim. Cosmochim. Acta*, 2003, **67**(20), 3937–3942.
39 S. Hashimotet, Y. Tatsuno and T. Kitagawa, *J. Am. Chem. Soc.*, 1987, **109**, 8097–8098.
40 R. L. Frost, A. W. Musumeci, W. N. Martens, M. O. Adebajo and J. Bouzaid, *J. Raman Spectrosc.*, 2005, **36**, 925–931.
41 H. J. Mathieu and D. Landolt, *Corros. Sci.*, 1986, **26**, 547–559.
42 R. V. Siriwardene and J. M. Cook, *J. Colloid Interface Sci.*, 1985, **108**, 414–422.
43 B. J. Tan, K. J. Klabunde and P. M. A. Sherwood, *Chem. Mater.*, 1990, **2**, 186–191.
44 B. A. Manning, J. R. Kiser, H. Kwon and S. R. Kanel, *Environ. Sci. Technol.*, 2007, **41**, 586–592.
45 L. Z. Zhang, Z. H. Ai, Y. Cheng and J. R. Qiu, *Environ. Sci. Technol.*, 2008, **42**, 6955–6960.
46 O. Masaoki and H. Kichinosuke, *J. Electron Spectrosc. Relat. Phenom.*, 1976, **8**(5), 475–481.
47 P. S. Nico, B. R. Stewart and S. Fendorf, *Environ. Sci. Technol.*, 2009, **43**, 7391–7396.
48 H. E. Roberts, K. Morris, G. W. Law, J. F. W. Mosselmans, P. Bots and K. S. S. Kvashnina, *Environ. Sci. Technol. Lett.*, 2017, **4**, 421–426.
49 Y. Hu, Q. Xue, J. Tang, X. Fan and H. H. Chen, *Chemosphere*, 2019, **222**, 511–516.